

Observations of the auroral width spectrum at kilometre-scale size

N. Partamies¹, M. Syrjäsuo¹, E. Donovan², M. Connors³, D. Charrois⁴, D. Knudsen², and Z. Kryzanowsky²

¹Finnish Meteorological Institute, Helsinki, Finland

²Institute of Space Research, University of Calgary, Calgary, Alberta, Canada

³Athabasca University, Athabasca, Alberta, Canada

⁴Syzygy Research & Technology, Legal, Alberta, Canada

Received: 21 September 2009 – Revised: 14 February 2010 – Accepted: 4 March 2010 – Published: 9 March 2010

Abstract. This study examines auroral colour camera data from the Canadian Dense Array Imaging SYstem (DAISY). The Dense Array consists of three imagers with different narrow (compared to all-sky view) field-of-view optics. The main scientific motivation arises from an earlier study by Knudsen et al. (2001) who used All-Sky Imager (ASI) combined with even earlier TV camera observations (Maggs and Davis, 1968) to suggest that there is a gap in the distribution of auroral arc widths at around 1 km. With DAISY observations we are able to show that the gap is an instrument artifact and due to limited spatial resolution and coverage of commonly used instrumentation, namely ASIs and TV cameras. If the auroral scale size spectrum is indeed continuous, the mechanisms forming these structures should be able to produce all of the different scale sizes. So far, such a single process has not been proposed in the literature and very few models are designed to interact with each other even though the range of their favourable conditions do overlap. All scale-sizes should be considered in the future studies of auroral forms and electron acceleration regions, both in observational and theoretical approaches.

Keywords. Ionosphere (Auroral ionosphere; Instruments and techniques) – Magnetospheric physics (Auroral phenomena)

1 Introduction

Ground-based imaging of the auroral engages a full family of optical instruments. The currently largest networks, Magnetometers – Ionospheric Radars – All-sky Cameras

Large Experiment (MIRACLE) (Syrjäsuo et al., 2001) in Fennoscandian and Svalbard and NORthern Solar Terrestrial ARray (NORSTAR) (Donovan et al., 2003) and Time History of Events and Macroscale Interactions during Substorms (THEMIS) (Donovan et al., 2006) in Canada and Alaska, consist of all-sky cameras (ASC). These imagers are designed for automatic long-term observations and include both colour and whitelight cameras, as well as systems with filter wheels and filters for certain auroral emission wavelengths. Fish-eye optics of ASCs allow monitoring the full sky at once. The spacial resolution (although dependent on the size of the Charge Coupled Device (CCD)) is typically at its best when observing meso-scale auroral structures of about 10–100 km with a temporal resolution of about 3–20 s. Narrow field-of-view (FoV) imagers are more often operated during campaigns only. They tend to aim for TV rate imaging with 25 or 30 frames per second (e.g. Trondsen, 1998). The best performance for these devices is for observations of fine-scale auroral structures of the order of about 10–100 m. Some narrow FoV instruments are equipped with filters (e.g. Dahlgren et al., 2008) but high data rate on less sensitive cameras may also require non-filtered gray-scale imaging. This study uses colour images and the results are compared with both non-filtered whitelight data (Maggs and Davis, 1968) as well as filtered images (Knudsen et al., 2001). A more detailed description on the available instruments at the moment and their capabilities and disadvantages in auroral imaging is given in a recent review by Sandahl et al. (2008).

As pointed out by Knudsen et al. (2001), the scale size region between the fine-scale (up to some hundreds of metres) and meso-scale (from about 10 km up) structures is not often monitored and reported in the literature. Because we are missing the imagers that easily resolve the auroral structures at and around 1 km scale size, this can be either an instrumental issue or a physical fact that these sizes do not occur as frequently as others. Although narrow electron acceleration



Correspondence to: N. Partamies
(noora.partamies@fmi.fi)

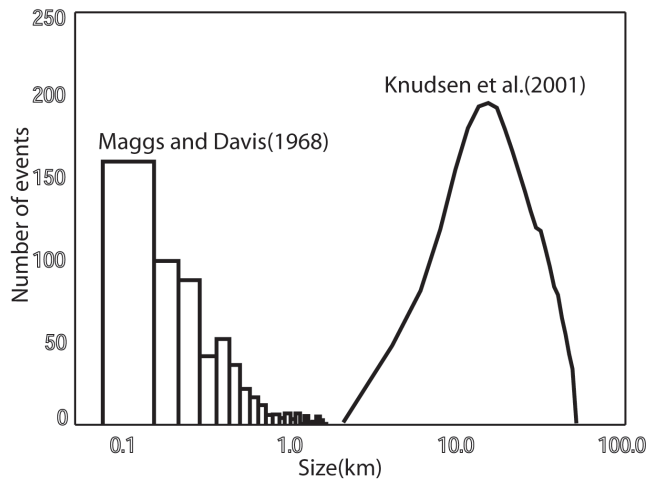


Fig. 1. Histograms of auroral arc widths as recorded by an all-sky imager (Knudsen et al., 2001) and a narrow FoV TV camera (Maggs and Davis, 1968). These histograms cover a very different scale size region due to the different instrumental specifications. The plot is according to Knudsen et al. (2001).

events were visible in the satellite data, the absence of optical arcs thinner than about 2 km was reported by Stenbaek-Nielsen et al. (1998). The question of existence or absence of these scale sizes is an important issue to examine in order to help the modelling work on auroral structures.

Furthermore, Knudsen et al. (2001) studied a set of 3126 meso-scale auroral arcs observed by the CANOPUS ASC in Gillam, Manitoba, Canada (Rostoker et al., 1995). They used images of the green auroral emission (wavelength of 557.7 nm) to identify auroral arcs. All arc images were analysed to find the arc widths, defined as full-width half-maximum (FWHM) values of the brightness profiles. For this purpose the arcs were mapped to the altitude of 135 km. The spatial resolution of the Gillam imager with a 200×200 -pixel Charge Coupled Device (CCD) was about 1.7 km in the zenith at the auroral altitudes. Their results showed that the typical auroral arc width is 18 ± 9 km with a sharp cutoff due to the instrument resolution at 3.4 km. These observations were compared with earlier TV camera results of 581 fine-scale auroral structures (Maggs and Davis, 1968). The widths of the fine-scale aurora range from 70 m (the minimum observable size of the TV camera) up to a few km with the median value of 230 m. The FoV of their instrument was $12^\circ \times 16^\circ$. Figure 1 is a replica from Knudsen et al. (2001) and shows the two frequently observed size ranges with a clear lack of arc width recordings in the middle. This plot demonstrates the need for observations optimised for 1 km scale size to determine whether the gap in the width distribution of auroral arcs suggested by these observations is real. Two separate arc width distributions would imply two different mechanisms to form auroral structures of different sizes, which would be an important insight into the search for the-

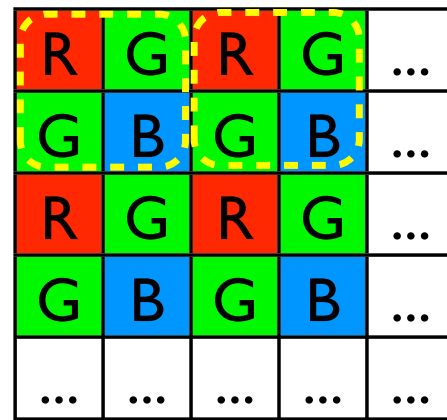


Fig. 2. Distribution of red, green and blue elements in the Bayer colour filter array. The yellow dashed lines circle the four-pixel groups that are used as grid points in the interpolation (colour synthesis).

oretical explanations for auroral arc formation. And if there is a physical reason for the absence of this scale-size in the aurora, it is of great importance to understand why this is and find out what prevents the electron acceleration to map continuously to all spatial scales.

Theoretical work by Chaston et al. (2003) provides an example of arc formation mechanism. They suggest that inertial Alfvén waves can drive 1 km wide auroral structures near the polar cap boundary. An earlier theoretical review by Borovsky (1993) showed that there are a number of mechanisms that would produce auroral structures with the minimum widths of 1–3 km. Examples of mechanisms that could potentially produce small-scale field-aligned electric fields in the acceleration region are double layers (e.g. Borovsky, 1988), particle anisotropies (e.g. Mauk, 1989) and anomalous resistivity (e.g. Stasiewicz, 1984). The next challenge would be to look at the theoretical work together with the full spectrum of observed auroral structures.

2 DAISY imagers

DAISY consists of three imagers operating at the visible wavelengths: one with a FoV of 20° and two with FoVs of 90° . An infra-red filter with a bandpass of 400–700 nm is used to block the longer wavelengths and help focussing (IR focus point is different from the visible one). A recently developed approach to auroral imaging is to use an off-the-shelf sensitive colour CCD. The device incorporates a Bayer colour filter array integrated onto the sensor (Sony Corporation, 2003). A sketch of the colour matrix with the locations red, green and blue (RGB) colour elements is drawn in Fig. 2. A colour synthesis step is required to decode the colour information for a final colour image. We used a simple nearest-neighbour averaging to obtain RGB values at each four-pixel

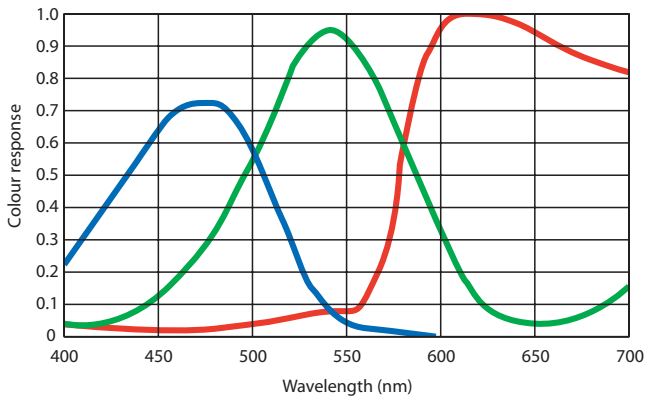


Fig. 3. Colour responses of the wide-band blue, green and red (maxima left to right) channel of the Bayer colour matrix. These curves are reconstructed from the data sheet given by the manufacturer.

group. The response functions of the wide-band colour channels in red, green and blue are illustrated in Fig. 3. The colours here refer to the wavelength region where the maximum sensitivity is. Some more technical details of DAISY can also be found in Partamies et al. (2008). Because the colour channels are wide, exact information on a particular emission line cannot be deduced. It has been shown, however, that when the background illumination is negligible the wide band colour channels can be fitted to calibrated photometric measurements of narrow emission lines of auroral red (630.0 nm), green (557.7 nm) and blue (427.8 nm) with relative errors as small as 10–20% (Partamies et al., 2007). Thus, some spectral information can be resolved also from the beautiful colour images.

The full resolution undecoded images read from the CCD are 1000×1000 pixels with 16-bit dynamic range. After colour synthesis, the final images are 500×500 pixels (see, lower panel in Fig. 5), and thus, the average spatial resolution is about 100 m (a minimum observable size). An ultimate upper limit for an observable size has to be smaller than $500 \text{ pixels} \times 100 \text{ m/pixel} = 50 \text{ km}$.

3 Colour data

The data for this study were recorded at the Athabasca University Geophysical Observatory (AUGO, 62.0° CGMLAT) in Alberta, Canada mainly from mid-January until the end of March 2007. This was the first campaign with DAISY fully in operation; in this study we only use data from the 20° FoV DAISY imager, which was designed for studies of kilometre sizes. This camera was pointed up along the local magnetic field line with the zenith angle 13.24° and the azimuth angle 17.7° at AUGO. A sketch of the viewing geometry is shown in Fig. 4. Because the camera is viewing the plane of auroral altitude (135 km) at an angle, along the magnetic field, the pixels closer to the zenith comprise a smaller physical

area than the ones at the edge of the southward FoV. We estimate this effect by calculating the size of each pixels at the image plane separately. The sizes vary from 94 to 112 m. Thus, the effect of pixel stretching is negligible compared to the measured widths of the auroral structures. The other two cameras at neighbouring stations to the north and south of AUGO provide an opportunity for altitude profile studies of auroral emissions, which will be utilised in future studies.

Thin arc-like structures were recorded during eight clear and active nights. The most eventful night was on 24 March 2007 around the magnetic midnight ($\sim 21:00$ – $04:00$ MLT, or $05:00$ – $12:00$ UT). Figure 5 shows four images taken during this night. The upper row images are from a colour all-sky camera (Syrjäsuo et al., 2005; Partamies et al., 2007), and the lower ones are from the DAISY camera, both at AUGO. In DAISY images, thin auroral structures are clearly visible.

An additional data set of 31 arc-like structures has been analysed from the DAISY prototype data (Partamies et al., 2008). The prototype was tested in Churchill, Manitoba (68.6° CGMLAT), for a week in March 2005. It had optics for a 60° FoV and thus, a spatial resolution of about 300 m at the auroral altitudes.

It is evident that also the exposure time has an effect on the width of the auroral structures as seen in the images. The DAISY exposure times are chosen to be just long enough to obtain a reasonable signal-to-noise ratio, but on the other hand short enough to result in as little motion blurring as possible. We used an exposure time of four seconds and an image cadence of 12 s. The 12-s cadence was selected to be a multiple of the imaging interval used in the Time History of Events and Macroscale Interactions During Substorms (THEMIS) (Donovan et al., 2006) cameras. Simultaneous all-sky images from the surrounding stations help in bringing the finer-scale structures into a larger context. For instance, a drift velocity of about 100 m/s in the north–south direction would result in a 100 m wide arc to blur into a 400 m wide structure during the exposure. Most of the observed structures (and the fine-scale intensifications in them) moved fast in the east–west (along the arc) direction, so that the width measurement was typically possible only in 1–3 images before the structure disappeared. In the north–south (across the arc) direction the arc motion was rather slow, whenever the structure stayed in the FoV long enough for this motion to be observed. So the blurring effect due to north–south drift is assumed to be minor. Fine-scale structures, such as curls and ripples, moving along the thin arcs did occur, but their impact to the statistical arc width is negligible as the locations for the arc width measurements were manually selected.

4 Thin arc statistics

During early 2007 we captured about 500 thin arc-like structures. These were mainly observed during eight nights, in different magnetic conditions. The planetary K_p index value

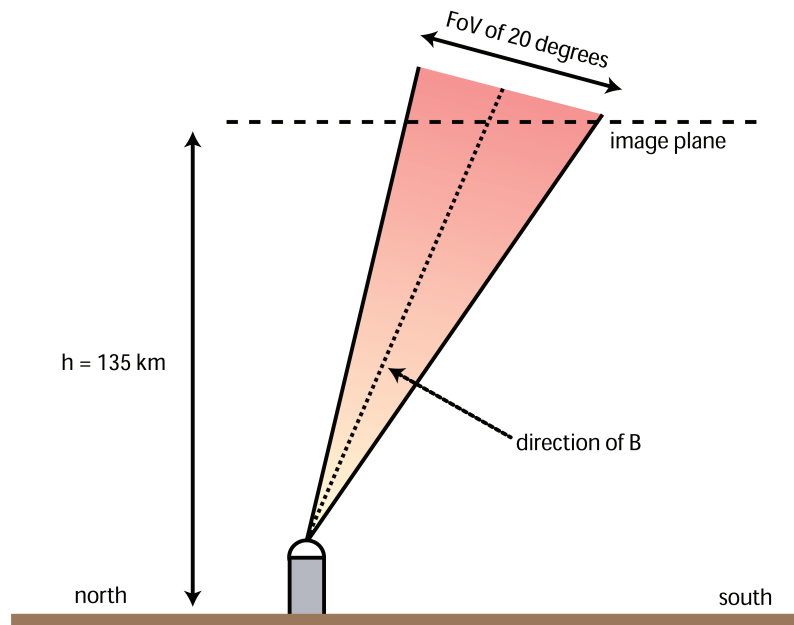


Fig. 4. A sketch of the FoV and its geometry. The camera is pointed in the direction of the local magnetic field with the zenith angle of 17.7° .

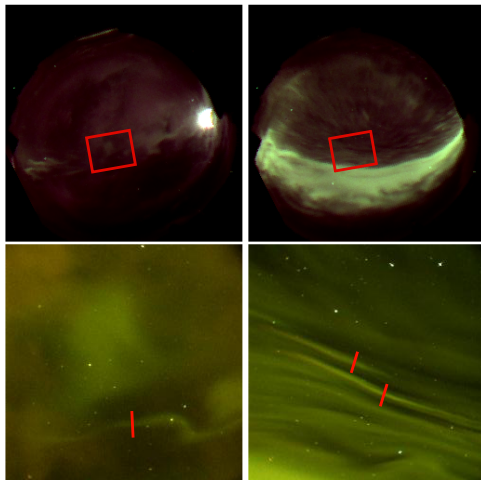


Fig. 5. Two examples of the DAISY images (lower panel) from the unit with the narrowest FoV. The images in the top panel are from an all-sky camera at AUGO. The red squares in the top panel images denote the approximate FoV of the DAISY images. Thin auroral structures can be seen in found in both images. Exposure time of 4 s was used to capture these at 05:49:36 (left column) and 08:18:48 UT (right column) on 24 March 2007. The thin structure in the image on the left hand side is a folded one, and the aurora (green) is partly behind some thin clouds (orange). In the image on the right, two almost straight arc-like structures are seen as brighter lines across the FoV. The widths measured from these images are 1.2 km (left), and 1.0 and 1.4 km (right) along the red lines across the structures. North is to the top and east to the right in these images.

ranged from 3 to 5 and the lower curve of the auroral electrojet index (AL) varied from 0 to -1400 nT during the auroral nights. Locally, these thin auroral structures were associated with both quiet conditions as well as substorm growth, expansion and recovery phases. About 10% of the thin structures occurred clearly outside of substorm-type activity, and another 10% of the events were closely related to substorm onset. Furthermore, about 70% of the thin structures were captured in the pre-midnight magnetic local time sector, and the rest in the post-midnight hours.

Every image and every thin structure was analysed separately. Thus, some of these structures may have been identified in 2–3 consecutive images, but in these scale sizes aurora evolves so quickly that it would be very difficult and highly ambiguous to try to decide whether a thin feature in an image is the same as the one seen in the previous image.

After the thin structures were identified in the images, their brightness profiles were analysed to determine the width of the structure. We define the widths the same way as Knudsen et al. (2001) did in their study. We take the brightness profiles along the cross-section of the aurora, and then rotate the cross-section line to find the minimum width. Examples of thin auroral structure in DAISY data is shown in the lower panel of Fig. 5. The red lines in the image on the lower right hand side corner mark the analysed cross-section of the arc.

Fitting a Gaussian function to the brightness profiles at the thinnest spots of the structures (Fig. 6) gives us a full-width half-maximum (FWHM) value that is taken as an estimate of the width of the structure. The Gaussian curve is expressed as

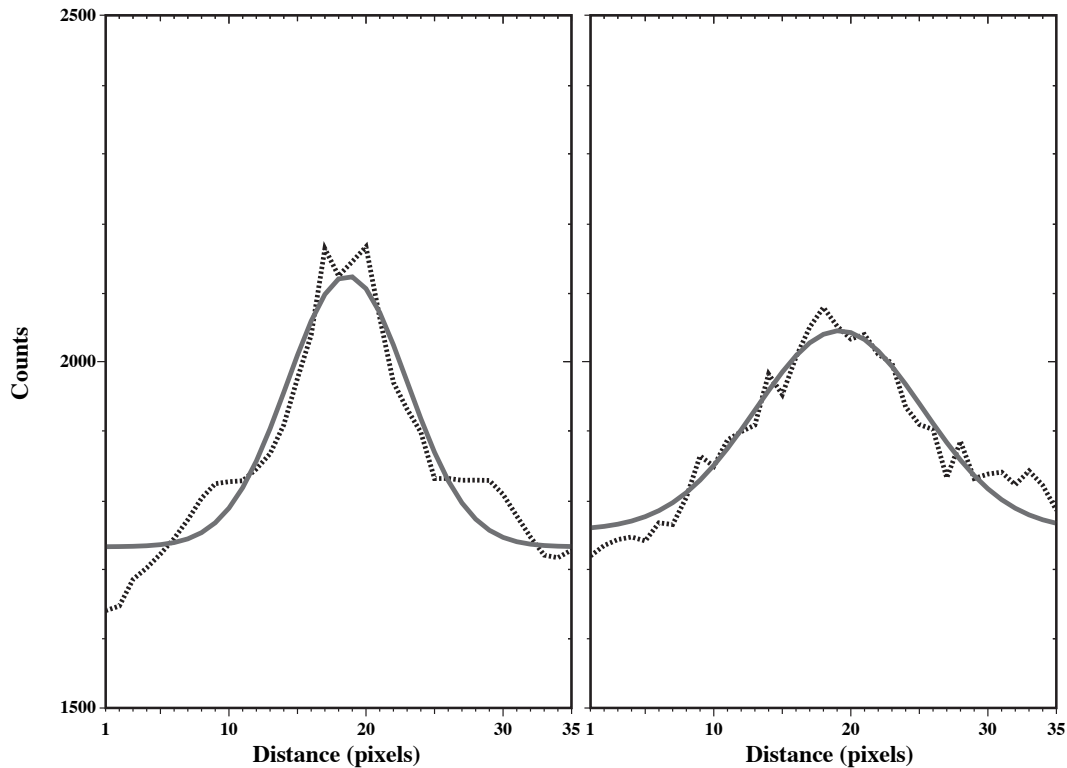


Fig. 6. The relative brightness (dashed lines) plotted along the two red cross-section lines drawn in the lower right image of Fig. 5. The solid gray lines show the Gaussian fit to the brightness profile. The FWHM of these sample structures at the altitude of 135 km are 1.0 and 1.4 km (~10 and 14 pixels, respectively).

$$y = A_1 \exp(-(x - A_2)^2 / 2A_3^2) \tag{1}$$

where A_1 is the amplitude of Gaussian, A_2 is the position of its maximum, and A_3 is FWHM. The residual normalised to the arc amplitude (intensity) was defined as

$$R = \sqrt{\Sigma((y - m)^2)} / A_1 \tag{2}$$

where y is the fitted Gaussian value and m gives the corresponding value of the measured profile. All events agreed very well with the Gaussian function with residuals clearly less than 10%. The conversion from pixels to kilometers is based on star calibration: one pixel corresponds to about 100 m at the altitude of 135 km.

In this study, we have defined the brightness to be simply the average of the four-pixel cell colour components (R, B and 2G as seen in Fig. 2). Thus, one may wonder what is the role of separate colour components in the observed widths. In Fig. 7 we have saved the RGB components from the raw colour image and fitted them separately. Due to the wide colour response functions (Fig. 3) the red channel gives a structure almost identical to that of the green one. This is due to the fact that the auroral green emission (557.7 nm) is close to yellow wavelengths (570–580 nm), and thus, consists of components in red and green ($R + G = Y$). Very little

emission is recorded at the blue wavelengths. Most importantly, the fitted width values are 1.0, 1.0 and 0.9 km for R, G and B, respectively, i.e. almost the same. Consequently, using the averaged brightness profiles of the full colour images will provide FWHM values that represent the auroral events very well for statistical purposes.

The auroral widths obtained in this study are shown in Fig. 8 (red) together with the previous statistics by Knudsen et al. (2001) (blue) and Maggs and Davis (1968) (black). The sizes of our 500 thin structures range from about 400 m to 7.5 km. The typical thickness was 0.5–1.5 km, where about 70% of the events sit. Our observations do not show any clear dependence of the width on the local time. Most of the DAISY observations contain auroral structures within the gap between the two previous distributions with some overlap with the results from the two previous studies. An additional small set of events from the DAISY prototype imager (green) cover the scale range from a few kilometres up to about 10 km. The DAISY prototype data have somewhat lower resolution and a larger FoV (60°) giving an observable size larger than the final DAISY instruments. The DAISY prototype histogram, although not in the main set of observations, has a more Gaussian shape than the records from the DAISY proper and the ones by Maggs and Davis (1968). This is probably only due to the very small amount of events

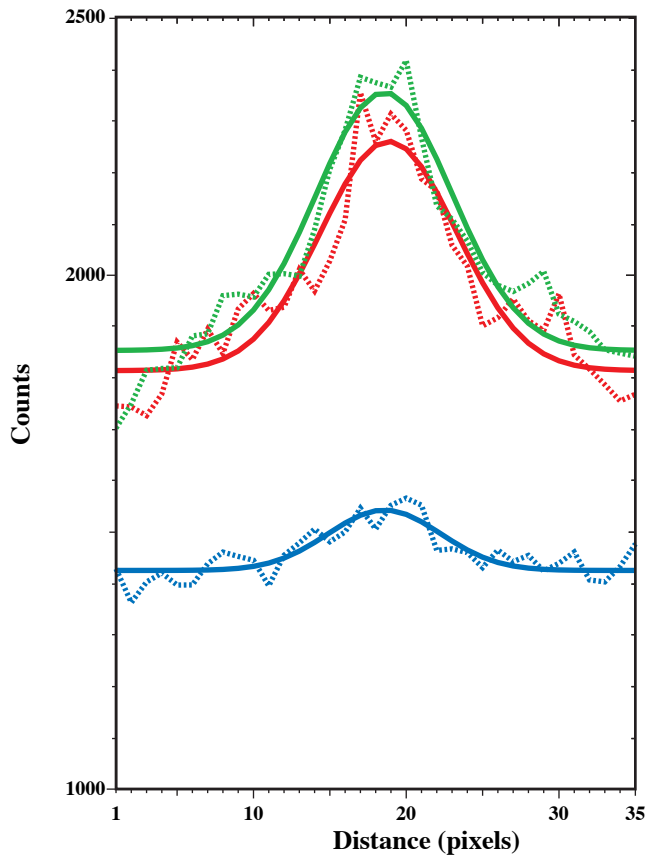


Fig. 7. The arc brightness curves (dashed lines) along the 1 km cross-section line in the lower right image of Fig. 5 for green, red and blue colour separately (24 March 2007, at 08:18:48 UT). The solid lines are the corresponding Gaussian fits to the brightness profiles. The FWHMs are 1.0 (R), 1.0 (G) and 0.9 km (B).

and similar activity conditions. The widths we are able to resolve do depend on the spatial resolution of the instrument – with the same CCD, the resolution decreases with increasing FoV. The prototype arc observations are included in this study (green histogram) to demonstrate this effect.

5 Summary and conclusions

We have used a new auroral colour imaging instrument called Dense Array Imaging SYstem (DAISY) to study small-scale auroral structures. The DAISY imager with the narrowest FoV (20°) was designed to have high enough spatial resolution to resolve auroral structures of 1 km scale size. So far very few observations in that scale size are found in the literature and no statistical set of observations has been reported. The previous study by Knudsen et al. (2001) brought up a question whether 1 km wide structures commonly exist in the aurora and have simply not been observed because of the inappropriate resolution of the available imagers. Alternatively, these structures are indeed absent because of the

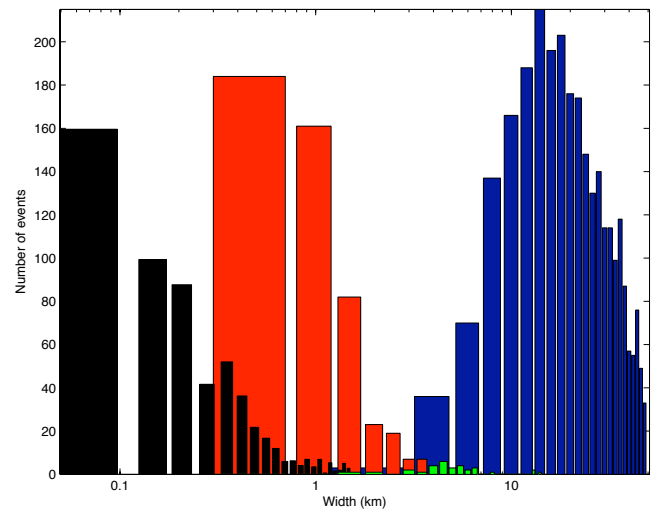


Fig. 8. Histograms of the scale sizes of the auroral structures. The black one is from the statistics of Maggs and Davis (1968), the red bars illustrate the results from this study, and the scale sizes from the all-sky data by Knudsen et al. (2001) are shown in blue. The tiny green bars denote the widths from the Dense Array prototype observations.

mechanisms that produce auroral arc-like structures are not capable of forming these widths. Our results support the continuous scale-size spectrum. The median arc width (0.5–1.5 km) and the observed width range (400 m–7.5 km) in this study are similar to the findings of (Chaston et al., 2003). The smallest structures found in this study are at the edge of the measurable range and the sharp cut-off is likely to be affected by instrumental artifacts.

This study reports the results of the analysis of 500 thin auroral structures from the DAISY images. The widths of these structures are estimated by fitting a Gaussian function to the brightness profile of each and every arc-like structure. The fitted FWHM value gives an estimate of the thickness of the thin auroral arc. About 70% of the thin structures seen in the DAISY images are 0.5–1.5 km wide, and the full size distribution fills most of the unobserved scale size space between the previous fine-scale observations by Maggs and Davis (1968) and the meso-scale statistics by Knudsen et al. (2001). The size range that is currently least observed is around a few kilometres. Available observations in this scale are from DAISY prototype with 60° . Although they comprise only a small amount of events compared to the other data sets, they fit and fill in the region between narrow FoV and all-sky observations. Together with the previous publications, this study shows that the typically observed scale size strongly depends on the spatial resolution of the available instrumentation – a fact that was already discussed by Borovsky et al. (1991). In addition, these findings suggest that the auroral scale size spectrum is, indeed, continuous rather than two separate distributions, which is

in a good agreement with the satellite measurements of narrow (<2 km) electron acceleration events (Stenbaek-Nielsen et al., 1998).

As pointed out by Semeter et al. (2008), already a few degrees off the magnetic zenith can cause a significant error in the width measured from the image. This is especially true for fine-scale aurora. They estimated the aspect angle error by assuming a horizontal size of 100 m and a vertical extent of 10 km for 10 keV electron precipitation. This results in a 1-to-100 ratio and thus, 100% relative error for structures that are located just 1% degree off the zenith. For our horizontal scale-sizes of about 1 km, the corresponding error would be about 10% per one degree offset. The median off-zenith-angle of the thin structures present here is 5°. According to the above reasoning, this would correspond to an error up to about 50% in the width estimates, which would shift the resulting histogram but would still not alter our conclusions. Furthermore, the 1-to-100 ratio assumes both vertical and horizontal brightness values to be constant, which is not what the auroral rays are. The instrumental and viewing angle effects are definitely something to keep in mind but not likely to be an issue in this study.

While our study demonstrates the existence of kilometre-scale arc structures, one must exercise caution in comparing directly with the larger and smaller structures reported in the two previous studies. The original Maggs and Davis (1968) structures were later attributed to the diffuse aurora (Stenbaek-Nielsen et al., 1999), whereas Knudsen et al. (2001) noted that the stable meso-scale arcs tended to occur in the pre-midnight sector and in the main auroral distribution, consistent with the fact that broad, stable arcs are typically seen prior to substorm onset. The narrower, more rapidly-changing structures reported in the present study were observed to occur predominantly in the pre-midnight sector and during geomagnetic conditions with $K_p=3-5$. They were captured both before and after substorm onsets, and even outside substorm activity. This suggests that the smaller scales are present in the substorm aurora but they may also co-exist with the stable, pre-breakup arcs, but were simply not visible with the Gillam ASC (Knudsen et al., 2001). Simultaneous multi-scale studies will have to be conducted to reveal the relative occurrence rate and probability of different scale-sizes, and their selection and interchange with changing magnetic activity.

Twelve electron acceleration mechanisms (e.g. wave-particle interactions and double layers) and ten generator mechanisms (e.g. shear flows at the boundary layers) that have been suggested to produce auroral arcs were evaluated by Borovsky (1993). The arc width predictions of these processes range from 0.7 to 340 km. No mechanism was found to form fine-scale structures as narrow as 100 m, and no mechanism was found to produce auroral arcs without scale size limitations. Ten out of these 22 mechanisms could produce arc thicknesses of 1–3 km, most of which take place in the near-Earth region rather than further out in the

magnetospheric boundary layers. So, there are both observations of the 1 km scale sizes in the aurora and a number of good candidates for their formation. But as it turns out that the auroral scale size spectrum is continuous, we suggest that the mechanism responsible for the formation of these structures should be able to produce the entire size range. To the best of our knowledge no such process has been reported in the literature. Thus, the future studies should seek for the multi-scale coupling of the different arc production mechanisms to support the multi-scale observations of the aurora, rather than concentrate on explaining one particular narrow range of widths in the auroral structures.

Acknowledgements. The work of N.P. has been funded by the Academy of Finland, the Alberta Ingenuity Fund, the Canadian Space Agency, and the Ministry of Education through the Finnish Graduate School in Astronomy and Space Physics. M.S. was financially supported by the Canadian Space Agency. The Dense Array Imaging SYstem development was supported by the Canada Foundation for Innovation. We also thank the Churchill Northern Studies Centre for hosting the DAISY prototype testing.

Topical Editor K. Kauristie thanks C. Chaston and another anonymous referee for their help in evaluating this paper.

References

- Borovsky, J.: Properties and dynamics of the electron beams emanating from magnetized plasma double layers, *J. Geophys. Res.*, 93, 5713–5725, 1988.
- Borovsky, J.: Auroral arc thicknesses as predicted by various theories, *J. Geophys. Res.*, 98, 6101–6138, 1993.
- Borovsky, J. E., Suszcynsky, D. M., Buchwald, M. I., and DeHaven, H. V.: Measuring the thicknesses of auroral curtains, *Arctic*, 44, 231–238, 1991.
- Chaston, C. C., Peticolas, L. M., Bonnell, J. W., Carlson, C. W., Ergun, R. E., McFadden, J. P., and Strangeway, R. J.: Width and brightness of auroral arcs driven by inertial Alfvén waves, *J. Geophys. Res.*, 108, SIA 17-1, 1091, doi:10.1029/2001JA007537, 2003.
- Dahlgren, H., Ivchenko, N., Sullivan, J., Lanchester, B. S., Marklund, G., and Whiter, D.: Morphology and dynamics of aurora at fine scale: first results from the ASK instrument, *Ann. Geophys.*, 26, 1041–1048, 2008, <http://www.ann-geophys.net/26/1041/2008/>.
- Donovan, E. F., Trondsen, T. S., Cogger, L. L., and Jackel, B. J.: All-sky imaging within the Canadian CANOPUS and NORSTAR projects, *Sodankylä Geophysical Observatory publications*, 92, 109–112, 2003.
- Donovan, E., Mende, S., Jackel, B., Frey, H., Syrjäsuo, M., Voronkov, I., Trondsen, T., Peticolas, L., Angelopoulos, V., Harris, S., Greffen, M., and Connors, M.: The THEMIS all-sky imaging array – system design and initial results from the prototype imager, *J. Atmos. Terr. Phys.*, 68, 1472–1487, 2006.
- Knudsen, D. J., Donovan, E. F., Cogger, L. L., Jackel, B. J. and Shaw, W. D.: Width and structure of mesoscale optical auroral arcs, *Geophys. Res. Lett.*, 28, 705–708, 2001.
- Maggs, J. E. and Davis, T. N.: Measurements of the thicknesses of auroral structures, *Planet. Space Sci.*, 16, 205–209, 1968.

- Mauk, B. H.: Generation of macroscopic magnetic-field-aligned electric fields by the convection surge ion acceleration mechanism, *J. Geophys. Res.*, 94, 8911–8920, 1989.
- Partamies, N., Syrjäsuo, M., and Donovan, E.: Using colour in auroral imaging, *Can. J. Phys.*, 85, 101–109, 2007.
- Partamies, N., Syrjäsuo, M., Donovan, E., and Knudsen, D.: Dense Array Imaging SYstem prototype observations of missing auroral scale sizes, in *Proceedings of the 33rd Annual Meeting on Atmospheric Studies by Optical Methods*, IRF Sci. Rep., 292, 95–101, http://www.irf.se/publications/proc33AM_files/partamies-et-al.pdf, 2008.
- Rostoker, G., Samson, J. C., Creutzberg, F., Hughes, T. J., McDiarmid, D. R., McNamara, A. G., Wallace Jones, A., Wallis, D. D., and Cogger, L. L.: CANOPUS – A ground based instrument array for remote sensing in the high latitude ionosphere during ISTPGGS program, *Space Sci. Rev.*, 71, 743–760, 1995.
- Sandahl, I., Sergienko, T., and Brändström, U.: Fine structure of optical aurora, *J. Atmos. Terr. Phys.*, 70, 2275–2292, 2008.
- Semeter, J., Zettergren, M., Diaz, M., and Mende, S.: Wave dispersion and the discrete aurora: New constraints derived from high-speed imagery, *J. Geophys. Res.*, 113, A12208, doi:10.1029/2008JA013122, 2008.
- Sony Corporation: ICX285AQ diagonal 11 mm (Type 2/3 CCD) progressive scan image sensor with square pixel for color cameras, <http://www.datasheetarchive.com/pdf/Datasheet-017/DSA00302749.pdf>, 2003.
- Stasiewicz, K.: On the origin of the auroral inverted-V electron spectra, *Planet. Space Sci.*, 32, 379–389, 1984.
- Stenbaek-Nielsen, H. C., Hallinan, T. J., Osborne, D. L., Kimball, J., Chaston, C., McFadden, J., Delory, G., Temerin, M., and Carlson, C. W.: Aircraft observations conjugate to FAST: Auroral arc thickness, *Geophys. Res. Lett.*, 25, 2073–2076, 1998.
- Stenbaek-Nielsen, H. C., Hallinan, T. J., and Peticolas, L.: Why do auroras look the way they do?, *Trans. Am. Geophys. Un. (EOS)*, 80, 193–199, 1999.
- Syrjäsuo, M. T.: FMI All-Sky Camera Network, *Geophysical Publications*, Finnish Meteorological Institute, ISBN 951-697-543-7, ISSN 0782-6087, 34 p., 2001.
- Syrjäsuo, M. T., Jackel, B. J., Donovan, E. F., Trondsen, T. S., and Greffen, M.: Low-cost multi-band ground-based imaging of the aurora, in *Proceedings of SPIE*, 5901, *Solar Physics and Space Weather Instrumentation*, edited by Silvano Fineschi, Rodney A. Viereck, 59010F1–11, 2005.
- Trondsen, T. S.: High Spatial and Temporal Resolution Auroral Imaging, Ph.D. thesis, University of Tromsø, Norway, available at http://www.phys.ucalgary.ca/~trondsen/Trondsen_Dissertation_1998/Trondsen_Dissertation_1998.pdf, 1998.